



P-200

## Deep Reservoirs Delineation by Swan's AVO Product Indicator: A Case Study

Hemalatha Kanta\*, Ashok Yadav, Jay Prakash Yadav, Ashutosh Garg, Reliance Industries Ltd.

### Summary

This paper describes Swan's methodology to generate AVO product indicator which is based on the deviations of AVO intercept  $A$  and gradient  $B$  values from the background trend. This indicator can be used to explore deeper hydrocarbon-bearing sands that are not detectable through conventional AVO attributes.

### Introduction

The success of AVO anomaly identification is constrained by the rock properties of the reservoir and its surrounding media. Class III anomalies are recognized as amplitude bright spots on stack data. The general product attribute  $AB$  indicates the presence of Class-III hydrocarbon bearing sands which are relatively shallow formations and have low acoustic impedance than the surrounding shale (Area1 in Fig 1). But the deeper hydrocarbon reservoirs which have nearly equal acoustic impedance with the surrounding shale, such as class II and class I sands are not detectable through the conventional product indicator  $AB$  (Area2 in Fig 1). Swan (1998) introduced a new attribute to delineate such type of reservoirs.

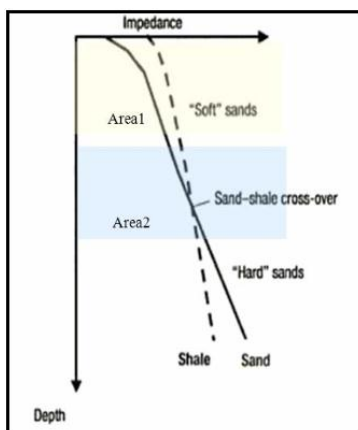


Fig 1: Schematic depth trends of sand and shale impedance

### Theory

Conventional AVO analysis performs a regression of the seismic signals in each NMO corrected gather to derive AVO intercept  $A$  and gradient  $B$  values at each time sample. Once this is done then the product of  $A$  and  $B$  is calculated as an AVO indicator.

The AVO product indicator describes the deviations of AVO intercept  $A$  and gradient  $B$  values from the background trend. AVO anomalies may then be detected by examining the deviations of data points from the fixed background region. This procedure is more amenable for scanning large quantities of data, since background reflections are automatically excluded from the consideration.

According to this attribute the important factor in AVO analysis is not the absolute variation of amplitude at each depth point but it is the relative variation with respect to background trend at each depth point.

### Methodology

First, generate AVO intercept value  $A$  and gradient value  $B$  for each depth point and convert them to their analytical (complex) form by adding the real trace ( $A_r(t), B_r(t)$  respectively) to  $i$  times of their Hilbert transform (Taner. et al. 1979). Then the statistics of  $A$  and  $B$  as function of time and space are generated from which deviations from the



background trend  $\Delta A$  and  $\Delta B$  are derived respectively for each depth point (explained in detail points 3 and 4 in the work flow). Then from  $\Delta A$ ,  $\Delta B$  the Swan's product indicator  $\Delta(AB)$  is derived, where  $\Delta(AB)$  is the deviation of  $AB$  from the background trend.

This indicator  $\Delta(AB^*)$  is phase independent since it utilizes the complex conjugate of AVO gradient so is not affected by any phase related problems.

The work flow is given as follows

1. Generate the analytical forms of AVO intercept  $A$  and gradient  $B$ .  
 $A(t) = A_r(t) + iH_i \{A_r(t)\};$   
 $B(t) = B_r(t) + iH_i \{B_r(t)\}.$   
 Where  $A_r(t)$ ,  $B_r(t)$  are the real AVO intercept and gradient traces respectively and  $H_i$  indicates the Hilbert transform.
2. Select the depth point ( $D_{pi}$ ) and window ( $W$ ) which surrounds the depth point ( $D_{pi}$ ) in time and CDP space, which is to be analyzed.
3. For the proper window selection derive some important statistics like RMS amplitudes " $\sigma_a$ " and " $\sigma_b$ " of  $A$  and  $B$  respectively and correlation coefficient " $r$ " over the window  $W$ .

$$\sigma_a = \sqrt{\frac{\sum_i W_i |A_i|^2}{\sum_i W_i}}$$

$$\sigma_b = \sqrt{\frac{\sum_i W_i |B_i|^2}{\sum_i W_i}}$$

$$r = \frac{1}{\sigma_a \sigma_b} \frac{\sum_i W_i A_i B_i^*}{\sum_i W_i}$$

Where ' $i$ ' is the  $i^{\text{th}}$  depth point within the window  $W$ ,  $|A_i|$ ,  $|B_i|$  are the magnitudes of  $A$ ,  $B$  at  $i^{\text{th}}$  depth point respectively and  $W_i$  is the weighing factor of the  $i^{\text{th}}$  depth point within the window  $W$  determined by

$$W_i = [A_i^2 + B_i^2]^{-Q}$$

Here  $Q$  is a weighing exponent which governs the relative contribution to the data statistics of strong and weak seismic reflectors.

4. Determine whether these statistics are well behaved over the window or not, for example, the values of AVO intercept  $A$  and gradient  $B$  are typically negatively correlated with each other. So the correlation coefficient " $r$ " should be a negative number close to  $-1$ . In addition, the values of " $\sigma_a$ " and " $\sigma_b$ " are analyzed to ensure that the points are not too scattered in  $A$ - $B$  plane. By this we can generate a background trend line with negative slope. If these QC conditions are not satisfied then the window size should be adjusted in time and CDP space accordingly.
5. Once the proper window is selected, Figure 2 shows how to derive  $\Delta A$ ,  $\Delta B$  and  $\Delta(AB)$ , the deviations of  $A$ ,  $B$  and  $AB$  from the background trend respectively, at each depth point.

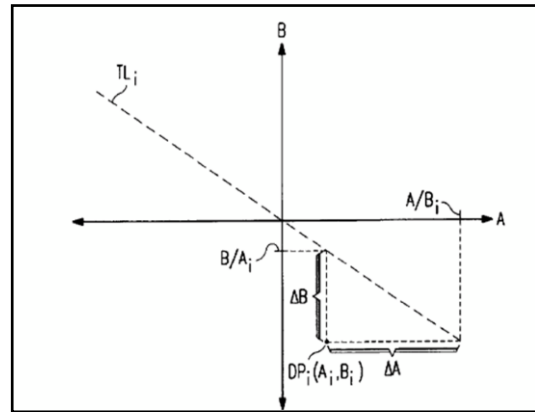


Fig 2: Method to derive the indicator  $\Delta(AB^*)$

$$\Delta A_i = A_i - A|B_i = A_i - B/C, \quad \Delta B_i = B_i - B|A_i = B_i - CA_i \text{ and}$$

$$\Delta(AB) = A_i \Delta B_i + B_i \Delta A_i.$$

where  $A|B_i$  is  $A$  given  $B_i$ ,  $B|A_i$  is  $B$  given  $A_i$  and the slope of the trend line  $TL_i$  is  $C$ .

## Case Study

### 1. Synthetic example

A synthetic example given in Figure 3 illustrates the concept introduced so far and showing the sand model of all classes and their amplitude responses in conventional product attribute  $AB$  as well as in the Swan's attribute  $\Delta(AB^*)$ .

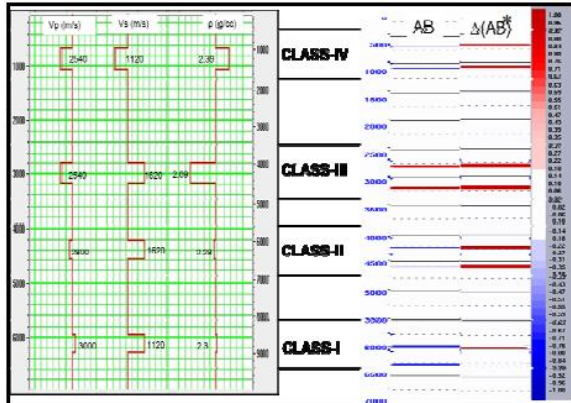


Fig 3: Sand model of all the classes and their amplitude responses in AB and  $\Delta(AB^*)$

It is observed that AB is showing positive anomaly only for class III sands. But  $\Delta(AB^*)$  is showing positive anomaly for all the sands irrespective of AVO class.

## 2. Seismic Example

### Background Geology

The basin of our interest is a Peri-Cratonic rift basin having horsts and graben structure conformable with basement morphology. The deposition of Tertiary sediments in this setup resulted in the formation of sedimentary prisms resting over the top of Cretaceous during Paleocene and later times.

Our zone of interest is mainly the Cretaceous sands, which are more compacted as compared to Tertiary sands. Thus these sands lie in Area 2 in Figure 1, where Class-III type of AVO response may not be expected.

## Results and Discussions

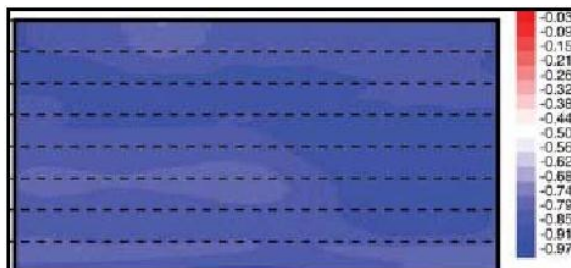


Fig 4: Correlation coefficient section between Intercept and Gradient

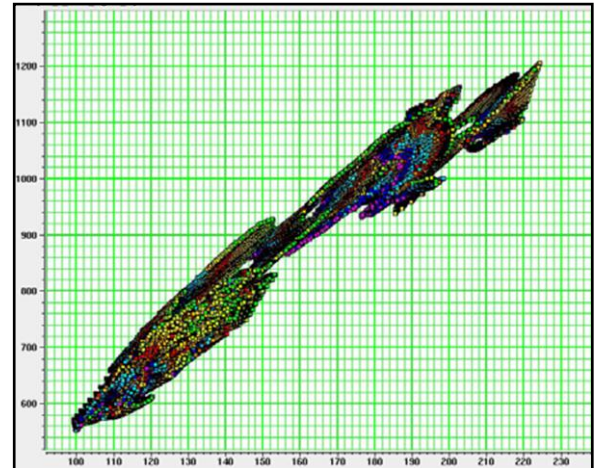


Fig 5: Crossplot between  $\sigma_a$  and  $\sigma_b$

Figures 4 and 5 show the Correlation coefficient (r) section and crossplot between " $\sigma_a$ " and " $\sigma_b$ " respectively these are the statistical characteristics of Intercept (A) and Gradient (B) to derive the Swan's attribute. As explained in point 4 in the work flow, correlation coefficient shows negative value (Figure4) close to -1 and there is no much scattering between  $\sigma_a$  and  $\sigma_b$  (Figure5).

Figure 6 shows the amplitude responses of conventional AVO product attribute AB and the corresponding  $\Delta(AB^*)$  attribute. Resistivity and P-impedance logs were overlaid on the Figures in black and red colors respectively.

Figures 6b, d, f, h and j are the  $\Delta(AB^*)$  responses corresponds to the conventional AVO product attribute AB of Figures 6a, c, e, g and i respectively.

In Figures 6b and d the encircled anomalous zones show positive AVO response in  $\Delta(AB^*)$  attribute where the conventional attribute AB in Figures 6a and c not show any anomalous behavior, although these areas have been verified by drilling to be gas bearing formations.

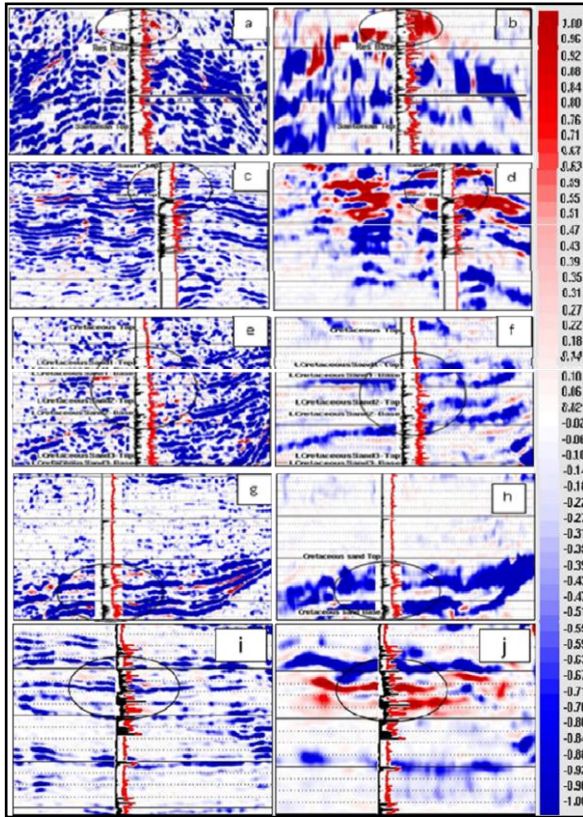


Fig 6: Comparison of conventional attributes AB (left) with the corresponding  $\Delta(AB^*)$  attributes (right)

On the other hand in the dry zones Figures 6e and g show a weak positive anomalous response in AB but not in Figures 6f and h correspond to  $\Delta(AB^*)$  attribute. However a deviation was observed in one case where  $\Delta(AB^*)$  shows positive signature (Figure 6j) and AB shows negative signature (Figure 6i) corresponds to a dry well.

Thus it is observed that the indicator  $\Delta(AB^*)$  is able to detect the presence of deeper hydrocarbon bearing sand formations that are undetectable by conventional AVO indicator in most cases.

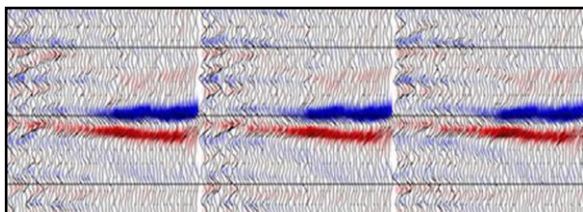


Fig 7: Phase rotated gathers (colour) overlaid on its corresponding original gathers (wiggles).

Figure 7 shows the phase rotated gathers (colour) overlaid on its corresponding original NMO corrected CDP gathers (wiggles) so that the farthest trace of phase rotated gather is  $90^\circ$  out of phase from its nearest trace in original gather.

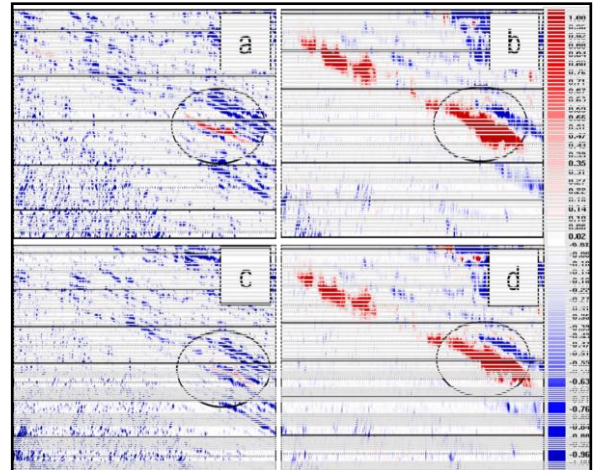


Fig 8: Comparison of AB of Original gathers and its phase rotated gathers (left) with its corresponding  $\Delta(AB^*)$  (right)

Figures 8b and d are the amplitude responses of Swan's attribute  $\Delta(AB^*)$  of original and its phase rotated gathers corresponds to the conventional attribute AB of Figures 8a and c respectively.

Well Name	Sand Type	Conventional Attribute (A*B)	Swan's Attribute $\Delta(AB^*)$	Discovery
A	Cretaceous Sand	No	Yes	Yes
B	Miocene Sand	Yes	Yes	Yes
C	Cretaceous Sand1	No	Yes	Yes
	Cretaceous Sand2	No	Yes	Yes
D	LCretaceous Sand1	No	No	No
	LCretaceous Sand2	No	No	No
E	LCretaceous Sand1	Weak	No	No
	LCretaceous Sand2	No	No	No
	LCretaceous Sand3	No	No	No
F	Oligocene Sand1	No	No	No
	LCretaceous Sand1	No	No	No
G	LCretaceous Sand1	No	No	No
	LCretaceous Sand2	No	No	No
H	Cretaceous Sand	Weak	No	No
I	Cretaceous Sand	Yes	Yes	No

Table 1: Results of Conventional attribute and Swan's attribute of nine wells

In the conventional attribute Figure 8c shows weak AVO response this is derived from phase rotated gather as compared to Figure 8a, which is derived from original



gather. But Figures 8b and d corresponds to Swan's attribute of original and its phase rotated gathers show same amplitude responses. From this it is observed that phase related problems may lead to amplitude artifacts so Swan's attribute may help in this scenario.

### Conclusions

From this study it is concluded that

1.  $\Delta (AB^*)$  can be used as a direct hydrocarbon indicator regardless of AVO class. It will however need conformance of geological concepts so that proper background trend is calculated for its successful implementation.
2. In anomalous regions we often observe some phase rotation which may result in some amplitude-related artifacts. In such cases phase independent attributes would serve to minimize the phase related problems.
3. Since  $\Delta (AB^*)$  is phase independent, it cannot distinguish between top and base of the reservoirs and have low temporal resolutions similar to the envelope function.
4. Though, the attribute  $\Delta (AB^*)$  is proved successful in most of the cases dealt here, nevertheless its proportional to fail (as illustrated in this paper) is also to be taken into consideration when such analysis is performed.

### References

Sena, A. G., and Swan, H. W., 1998, Method and system for detecting hydrocarbon reservoirs using amplitude versus offset analysis of Seismic Signals. U. S. Patent 5784334.

Swan, H. W., 2007, Automatic compensation of AVO background drift. The Leading Edge; December. 26; no. 12; p. 1528-1536.

Swan, H. W., 2006, Phase-independent product indicators for AVO reconnaissance, SEG Expanded Abstracts 25, 249.

Taner, M.T., Koehler, F., Sheriff, R.E., 1979, Complex seismic trace Analysis, Geophysics, June. 44, No.6, pp 1041-1063.

### Acknowledgements

I gratefully acknowledge Reliance Industries Limited Petroleum E&P for allowing us to publish these results and their careful reviews. Special thanks are owed to Artrii Banerjee and Jayakrishna Appani for their support.